



Heriot-Watt University  
Research Gateway

# Sonic horizon dynamics for quantum systems with cubic-quintic-septic nonlinearity

## Citation for published version:

Wang, Y, Cheng, Q, Guo, J & Wang, W 2019, 'Sonic horizon dynamics for quantum systems with cubic-quintic-septic nonlinearity', *AIP Advances*, vol. 9, no. 7, 075206. <https://doi.org/10.1063/1.5110578>

## Digital Object Identifier (DOI):

[10.1063/1.5110578](https://doi.org/10.1063/1.5110578)

## Link:

[Link to publication record in Heriot-Watt Research Portal](#)

## Document Version:

Publisher's PDF, also known as Version of record

## Published In:

AIP Advances

## Publisher Rights Statement:

© 2019 Author(s). All article content, except where otherwise noted, is licensed under a Creative Commons Attribution (CC BY) license (<http://creativecommons.org/licenses/by/4.0/>)

## General rights

Copyright for the publications made accessible via Heriot-Watt Research Portal is retained by the author(s) and / or other copyright owners and it is a condition of accessing these publications that users recognise and abide by the legal requirements associated with these rights.



## Take down policy

Heriot-Watt University has made every reasonable effort to ensure that the content in Heriot-Watt Research Portal complies with UK legislation. If you believe that the public display of this file breaches copyright please contact [open.access@hw.ac.uk](mailto:open.access@hw.ac.uk) providing details, and we will remove access to the work immediately and investigate your claim.

# Sonic horizon dynamics for quantum systems with cubic-quintic-septic nonlinearity

Cite as: AIP Advances 9, 075206 (2019); <https://doi.org/10.1063/1.5110578>

Submitted: 19 May 2019 . Accepted: 26 June 2019 . Published Online: 08 July 2019

Ying Wang , Quan Cheng, Jiyuan Guo, and Wei Wang 



View Online



Export Citation



CrossMark

## ARTICLES YOU MAY BE INTERESTED IN

[Enhancing image quality of ghost imaging by fuzzy c-means clustering method](#)

AIP Advances 9, 075006 (2019); <https://doi.org/10.1063/1.5079681>

[Controllable and tunable multiple optomechanically induced transparency and Fano resonance mediated by different mechanical resonators](#)

AIP Advances 9, 075105 (2019); <https://doi.org/10.1063/1.5094820>

[Design of broadband reflector at the visible wavelengths using particle swarm optimization](#)

AIP Advances 9, 075301 (2019); <https://doi.org/10.1063/1.5090287>

AVS Quantum Science

Co-published with AIP Publishing



Coming Soon!

# Sonic horizon dynamics for quantum systems with cubic-quintic-septic nonlinearity

Cite as: AIP Advances 9, 075206 (2019); doi: 10.1063/1.5110578

Submitted: 19 May 2019 • Accepted: 26 June 2019 •

Published Online: 8 July 2019



View Online



Export Citation



CrossMark

Ying Wang,<sup>1,2,a)</sup>  Quan Cheng,<sup>1,2</sup> Jiyuan Guo,<sup>1</sup> and Wei Wang<sup>1,2,3,b)</sup> 

## AFFILIATIONS

<sup>1</sup>School of Science, Jiangsu University of Science and Technology, Zhenjiang 212003, China

<sup>2</sup>Laboratory of Advanced Optics, Jiangsu University of Science and Technology, Zhenjiang 212003, China

<sup>3</sup>Institute of Photonics and Quantum Sciences, School of Engineering and Physical Sciences, Heriot-Watt University, Edinburgh EH14 4AS, United Kingdom

<sup>a)</sup>Electronic mail: wangying@just.edu.cn

<sup>b)</sup>Electronic mail: w.wang@hw.ac.uk

## ABSTRACT

We study the sonic horizon formation problem for quantum system incorporating septic nonlinearity, which is modeled by the nonlinear Schrödinger equation (NLSE) with nonlinearity up to septic order. Based on the F-expansion method combined with modulus-phase transformation, we derived the soliton solutions of such NLSE for the one-dimensional and three-dimensional scenarios, from which the sonic horizon formation dynamical variables are derived. We identify that the distribution of system flow velocity and sound velocity, which determine the occurrence of the sonic horizon, agree well with the corresponding quantities obtained from pure numerical evaluation, demonstrating the applicability of the theoretical approach adopted in this study.

© 2019 Author(s). All article content, except where otherwise noted, is licensed under a Creative Commons Attribution (CC BY) license (<http://creativecommons.org/licenses/by/4.0/>). <https://doi.org/10.1063/1.5110578>

## I. INTRODUCTION

Black hole-related problems are fascinating subjects in fundamental physical phenomena study. Among the various intriguing features, event horizon is a typical landmark for black hole. The interior of the horizon is the region of black hole where everything, including light cannot escape due to the strong gravitational pull. In recent years, as close analog of black hole, the sonic blackhole in ultracold atomic systems has drawn special attention. As pointed out by Unruh,<sup>1</sup> in a sonic black hole, the propagation of sound takes the role of traveling light, the sonic horizon is just the boundary between the supersonic flow and subsonic flow. Some quantum fluids, such as Bose-Einstein condensates (BEC) are the ideal choice for realizing the sonic black hole and studying black hole-related physics. Unlike the uncontrollability and unrepeatability of astrophysical black hole, quantum fluids can be easily manipulated by nonlinearity modulation of Feshbach resonance technique and system external trapping adjustment. Recently, experiments demonstrated the formation of the sonic black hole together with the associated Hawking radiation in elongated (one-dimensional) BEC.<sup>2,3</sup>

Usually, the formation of sonic black holes in quantum system involve drastic change of constituents density, so higher-order nonlinear effects have to be considered. Recent studies show that the higher-order nonlinear effects<sup>4,5</sup> with contribution up to septic order are present in many systems such as organic materials,<sup>6</sup> highly nonlinear media like dye solutions,<sup>7</sup> ferroelectrics,<sup>8</sup> chalcogenide glasses,<sup>9</sup> and colloids.<sup>10</sup> For BEC, the septic nonlinearity comes from inter-particle multi-body interaction in the system. Nowadays, with relatively more experimental and simulated study<sup>11</sup> of the sonic black hole, more precise analytical study for this phenomena and related topics calls for the corresponding nonlinear Schrödinger equation (NLSE) model<sup>12-19</sup> to incorporate nonlinearity up to septic order.

Prior experimental and simulation work on quintic, septic nonlinearity demonstrate that higher-order nonlinearity can regularize the soliton related dynamics and prevent the higher-dimension spatial solitons<sup>20-22</sup> from collapsing. However, compared to the relatively more analytical study of the NLSE incorporating only cubic nonlinearity, more strict theoretical investigation for the NLSE with nonlinearity up to quintic and even septic order are rather rare.

In this study, for a typical quantum system such as BEC where sonic black hole is to be formed, we first investigate one-dimensional NLSE modeling the evolution of the system incorporating full cubic-quintic-septic nonlinearity and harmonic trapping potential. Via the  $F$ -expansion method<sup>23–25</sup> with modified modulus-phase transformation, we derive the typical exact soliton solution of the NLSE for the cubic-quintic-septic nonlinearity, cubic-quintic, cubic cases respectively for comparison purpose. The obtained dark soliton solution for the cubic-quintic-septic nonlinearity, where sonic horizon can occur, is visually demonstrated. For the actual study of the three-dimensional BEC where sonic black hole can be studied more generally, based on the self-similar approach, we also derive the soliton-related evolution for the three-dimensional NLSE with cubic-quintic-septic nonlinearity where sonic horizon can form in a more general manner.

To validate our theoretical work, we calculate the sonic horizon dynamics by deriving the system flow velocity based on the analytical soliton solution obtained for the system incorporating full cubic-quintic-septic nonlinearity. We achieve good agreement between our analytically derived flow velocity and the flow velocity from pure numerical simulation.

This work is organized as follows. The next two sections demonstrate the theoretical NLSE model that incorporates cubic-quintic-septic nonlinearity and the methodology for deriving the sonic horizon-related analytical solutions of the NLSE for the one-dimensional and three-dimensional cases. Section IV calculates the sonic horizon related dynamical variables based on the analytical solutions derived. The last section gives concluding remarks.

## II. SOLITON DYNAMICS FOR ONE DIMENSIONAL NLSE WITH NONLINEARITY UP TO SEPTIC ORDER

Usually the typical one-dimensional BEC system, where the sonic horizon forms, is relatively easy to manipulate and analytically handle, and many typical settings like BEC in elongated harmonic trapping potential are quasi one-dimensional (Trapping potential  $U(x, y, z) = \frac{1}{2}(k_x x^2 + k_y y^2 + k_z z^2)$ , where  $k_y, k_z \gg k_x$ ). With nonlinearity up to septic order, the 1D NLSE takes the following form

$$i\hbar \frac{\partial \Psi(x, t)}{\partial t} + \frac{\hbar^2}{2m} \frac{\partial^2 \Psi}{\partial x^2} - kx^2 \Psi + (g_1 |\Psi|^2 + g_2 |\Psi|^4 + g_3 |\Psi|^6) \Psi = 0 \tag{1}$$

where  $k = \frac{1}{2} m \Omega^2$  ( $\Omega = \Omega_x$ ). Next, we show that Eq. (1) is analytically solvable with the expansion method. We proceed from the coupled modulus-phase transformation, that takes the following form,

$$x' = \sqrt{\frac{2m\omega}{\hbar}} \sigma(t') x, \tag{2a}$$

$$t' = \Omega t, \tag{2b}$$

$$\Psi(x, t) = \sigma^{1/2}(t') \exp\left[i \frac{\sigma'(t')}{\sigma(t')} x^2\right] \varphi(x', t') \tag{3}$$

Plugging Eq. (2) and (27) into Eq. (1), we transform equation as follows,

$$i\varphi_t + \sigma^2(t) \varphi_{xx} + \left[ \frac{k(t)}{\sigma^2(t)} + \frac{1}{4} \left( \frac{\sigma_t(t)}{\sigma(t)} \right)^2 - \frac{1}{4} \left( \frac{\sigma_t(t)}{\sigma(t)} \right)_t \right] x^2 \varphi + (g_1 \sigma(t) |\varphi|^2 + g_2 \sigma^2(t) |\varphi|^4 + g_3 \sigma^3(t) |\varphi|^6) \varphi = 0 \tag{4}$$

We then take the ansatz for  $\varphi$  in Eq. (4) as

$$\varphi(x, t) = v(x, t) e^{i\theta(x, t)}, \tag{5}$$

and plugging Eq. (5) into Eq. (4), we then obtain the equations for  $v(x, t)$  and  $\theta(x, t)$  as follows,

$$v\theta_t + \sigma^2(t)(v v_{xx} + v \theta_x^2) + \alpha(t) x^2 v + \beta_1(t) v^3 + \beta_2(t) v^5 + \beta_3(t) \sigma^2(t) v^7 = 0 \tag{6a}$$

$$v_t + \sigma^2(t)(2v_x \theta_x + v \theta_{xx}) = 0 \tag{6b}$$

where  $\alpha(t) = k(t)/\sigma^2(t) + \frac{1}{4}(\sigma_t(t)/\sigma(t))^2 - \frac{1}{4}(\sigma_t(t)/4\sigma(t))_t$ ,  $\beta_n(t) = -g_n \sigma^n(t)$  ( $n = 1, 2, 3$ ). Equation (6) is now transformed to the form from which the expansion method can be used. The expansion method is implemented through the formulation of the base-function  $G(\xi)$  with  $\xi = p(t)x + q(t)$ . The solutions of Eq. (6) are then expressed as

$$v(x, t) = h(t)G(\xi), \tag{7a}$$

$$\theta(x, t) = \Phi_2(t)x^2 + \Phi_1(t)x + \Phi_0(t) \tag{7b}$$

where  $G(\xi)$  is defined as

$$\left( \frac{dG(\xi)}{d\xi} \right)^2 = H(G) = a_8 G^8 + a_6 G^6 + a_4 G^4 + a_2 G^2 + a_0 \tag{8}$$

Plugging Eqs. (7) into Eqs. (6) and making use of Eq. (8), we reach a polynomial of  $x^i G^j \left( \frac{dG(\xi)}{d\xi} \right)^k$  ( $i, j, k$  are integers), setting the coefficient formula of each term to zero, we reach the following set of equations,

$$x^2 G^j(\xi) : \Phi_2'(t) + 4\sigma^2(t)\Phi_2^2(t) + \alpha(t) = 0, \tag{9a}$$

$$x G^j(\xi) : \Phi_1'(t) + 4\sigma^2(t)\Phi_2(t)\Phi_1(t) = 0, \tag{9b}$$

$$G^8(\xi) : 8\sigma^2(t)p^2(t)a_8 - g_3 \sigma^3(t)h^6(t) = 0, \tag{9c}$$

$$G^6(\xi) : 6\sigma^2(t)p^2(t)a_6 - g_2 \sigma^2(t)h^4(t) = 0, \tag{9d}$$

$$G^4(\xi) : 4\sigma^2(t)p^2(t)a_4 - g_1 \sigma(t)h^2(t) = 0, \tag{9e}$$

$$G^2(\xi) : 2\sigma^2(t)p^2(t)a_2 - \Phi_0'(t) = 0, \tag{9f}$$

$$x G'(\xi) : p'(t) + 4\sigma^2(t)\Phi_2(t)p(t) = 0, \tag{9g}$$

$$G'(\xi) : q'(t) + 2\sigma^2(t)p(t)\Phi_1(t) = 0, \tag{9h}$$

$$G(\xi) : h'(t) + 2\sigma^2(t)\Phi_2(t)h(t) = 0 \tag{9i}$$

we can see from Eqs. (9) that

$$\sigma(t)p(t) = C_0, \sigma(t)\Phi_1(t) = C_1, \tag{10a}$$

$$\sigma(t)h^2(t) = C_2, \tag{10b}$$

$$a_8 = \frac{g_3 C_2^3}{8C_1^2}, \tag{10c}$$

$$a_6 = \frac{g_2 C_2^2}{6C_1^2}, \tag{10d}$$

$$a_4 = \frac{g_1 C_2}{4C_1^2} \tag{10e}$$

where  $C_1, C_2$  are constants to be determined by the initial experiment setting of the system, also from Eqs. (10)  $a_8, a_6$  and  $a_4$  are constants expressed through the nonlinear interaction strength constants  $g_1, g_2$  and  $g_3$ . So  $a_2$  and  $a_0$  can be freely adjusted according to the specific nonlinear features of the solutions we are interested. For comparison purpose, we derive the typical nonlinear solution of Eq. (1) for three categorical orders of nonlinear interaction. we will identify the typical feature for the sonic horizon formation with septic order nonlinearity.

### A. Cubic-quintic-septic nonlinearity

Here, the septic order nonlinear interaction constant  $g_3 \neq 0$ . The base function  $G(\xi)$  in Eq. (8) is formulated as

$$H(G) = a_8 G^8 + a_6 G^6 + a_4 G^4 + a_2 G^2 + a_0 = a_8 (G^2 - A)^2 (G^2 - B)^2 \tag{11}$$

From Eqs. (10), we have

$$A = -\frac{g_2}{3g_3 C_2} + \sqrt{\frac{g_2^2}{3g_3^2 C_2^2} - \frac{g_1}{g_3 C_2^2}} \tag{12a}$$

$$B = -\frac{g_2}{3g_3 C_2} - \sqrt{\frac{g_2^2}{3g_3^2 C_2^2} - \frac{g_1}{g_3 C_2^2}} \tag{12b}$$

$$a_2 = \frac{g_2}{6C_1^2} \left( \frac{2g_2^2}{9g_3} - g_1 \right) \tag{12c}$$

$$a_0 = \frac{g_3 C_2^3}{8C_1^2} \left( \frac{g_1}{g_3 C_2^2} - \frac{2g_2^2}{9g_3^2 C_2^2} \right) \tag{12d}$$

For the situation where  $g_2/g_3 < 0$  and  $g_1/g_3 > 0$ ,  $A = a^2 > 0$ ,  $B = b^2 > 0$  ( $|a| > |b|$ ), from Eq. (8)

$$\frac{dG(\xi)}{(G^2 - a^2)(G^2 - b^2)} = a_8^{1/2} d\xi \tag{13}$$

Eq. (13) can be integrated to the following form,

$$\log \frac{(1 - G/2)^{1/2} (1 + G/b)^{1/b}}{(1 + G/a)^{1/a} (1 - G/b)^{1/b}} = 2a_8^{1/2} (b^2 - a^2) \xi \tag{14}$$

Since  $g_3 \gg g_2, a \sim b \sim g_2/g_3 \gg 1, G/a \ll 1$  and  $G/b \ll 1$ , expand the fractional in the logarithm function of the LHS of Eq. (14) to the second order terms  $(G/a)^2$  and  $(G/b)^2$ . Eq. (14) is analytically solvable under this scenario with the following solution

$$G(x, t) = \frac{2ab \tanh(2a_8^{1/2} (A - B)\xi)}{(A - B) + \sqrt{(A - B)^2 + 2(b^2/a^3 + a^2/b^3) \tanh^2(2a_8^{1/2} (A - B)\xi)}} \tag{15}$$

Plugging Eq. (15) into Eqs. (7a), (5), (27) and utilizing Eq. (10b), we get

$$\begin{aligned} |\psi(x, t)| &= \rho^{1/2}(t)\varphi(x, t) = \rho^{1/2}(t)h(t)G(x, t) \\ &= \frac{2C_2^{1/2} ab \tanh(2a_8^{1/2} (A - B)\xi)}{(A - B) + \sqrt{(A - B)^2 + 2(b^2/a^3 + a^2/b^3) \tanh^2(2a_8^{1/2} (A - B)\xi)}} \end{aligned} \tag{16}$$

which is of dark soliton type. Fig. 1 shows the plot of this solution  $|\psi|^2$  with cubic-quintic-septic nonlinearity. So typical dark soliton behavior exists for one-dimensional quantum system with nonlinearity up to septic order. We will show later the derivation of system flow velocity and sound velocity for such system from phase and modulus of  $\psi(x, t)$ , which demonstrate the formation of the sonic horizon.

### B. Cubic-quintic nonlinearity

When the septic nonlinearity is not taken into account, so that,  $g_3 = 0, a_8 = 0$ , and through the appropriate selection of  $\Phi_0(t)$  (which is a free parametric function as shown earlier) so that  $a_0 = 0$ , so the septic Eq. (11) reduces to the following form

$$H(G) = a_6 G^6 + a_4 G^4 + a_2 G^2 = k_6 G^6 ((G^2 - c)^2 - d) \tag{17}$$

where  $c = -\frac{a_4}{2a_6}, d = \frac{a_4^2}{4a_6^2} - \frac{a_6}{a_2}, k_6 = a_2$ . For  $d > 0$ , based on the formulation of  $G(x, t)$  in Eq. (8) and Eq. (17),  $G(x, t)$  takes the following analytical format

$$G(x, t) = \sqrt{\frac{1}{d^{1/2} \cosh(a_2^{1/2} \xi) + c}} \tag{18}$$

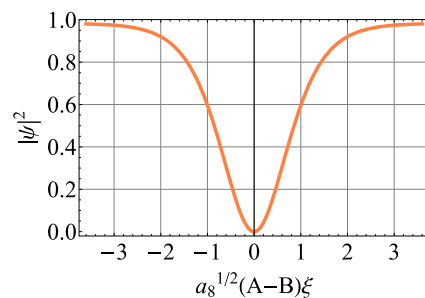


FIG. 1.  $|\psi|^2$  (in unit of  $\frac{4C_2 a^2 b^2}{((A - B) + \sqrt{(A - B)^2 + 2(b^2/a^3 + a^2/b^3)})^2}$ ) vs.  $a_8^{1/2} (A - B)\xi$  from Eq. (16) with cubic-quintic-septic nonlinearity.

The solution of the wave function for this case is

$$|\psi(x, t)| = C^{1/2} \sqrt{\frac{1}{d^{1/2} \cosh(a_2^{1/2} \xi) + c}} \quad (19)$$

which is of bright soliton type. Fig. 2 shows the plot of this solution  $|\psi|$  with cubic-quintic nonlinearity.

### C. Cubic nonlinearity

In this scenario,  $g_2 = g_3 = 0$ , such that  $a_8 = a_6 = 0$ . Eq. (1) is just the classic (1+1)-dimensional nonlinear Schrödinger equation (NLSE) with only cubic nonlinearity and harmonic trapping potential. Here, we just follow the line of analytical solution derivation based on the expansion approach and investigate the classic soliton solution of this category of cubic NLSE. To proceed, We choose two specific categories of polynomials for  $G$  in its formulation Eq. (8) regarding the value of  $a_0$ .

Case 1 ( $a_0 = 0$ ):

In this case,

$$H(G) = a_4 G^4 + a_2 G^2 = k_4 G^4 (G^{-2} - f) \quad (20)$$

where  $k_4 = a_2$ ,  $f = -\frac{a_4}{a_2}$ , when  $f > 0$ ,  $G(x,t)$  that satisfies  $\frac{dG(\xi)}{d\xi} = \sqrt{H(G)}$  has the following analytical solution:

$$G(x, t) = \sqrt{\frac{a_2}{a_4}} \operatorname{sech}(|a_2|^{1/2} \xi) \quad (21)$$

so

$$|\psi(x, t)| = C_2^{1/2} \sqrt{\frac{a_2}{a_4}} \operatorname{sech}(|a_2|^{1/2} \xi) \quad (22)$$

which is the solution of bright soliton type.

Case 2 ( $a_0 = \frac{a_2^2}{4a_4}$ ):

In this case,

$$H(G) = a_4 G^4 + a_2 G^2 + a_0 = a_4 (G^2 - u)^2 \quad (23)$$

where  $u = -\frac{a_2}{2a_4}$ . With  $u > 0$ ,  $G(x, t)$  has the following solution

$$G(x, t) = 2 \sqrt{\frac{a_2}{a_4}} \tanh(|2a_2|^{1/2} \xi) \quad (24)$$

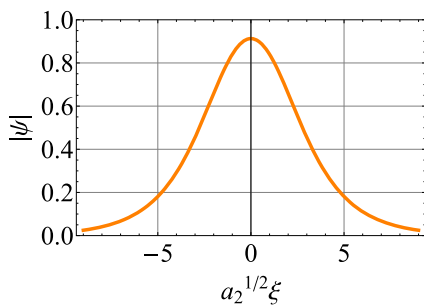


FIG. 2.  $|\psi|$  (in unit of  $C^{1/2}$ ) vs.  $a_2^{1/2} \xi$  from Eq. (19) for cubic-quintic nonlinearity with  $d = 0.01$  and  $c = 1.0$ .

so that  $|\psi(x, t)| = 2C_2^{1/2} \sqrt{\frac{a_2}{a_4}} \tanh(|2a_2|^{1/2} \xi)$  which is solution of dark soliton type. Besides those of (13) with quadratic forms (13), (17), (20) and (23), other nonlinear interaction constants values of  $g_1$ ,  $g_2$  and  $g_3$  (that determines  $a_4$ ,  $a_6$  and  $a_8$  respectively) will make  $H(G)$  take more general form. The analytical solutions for  $G(x, t)$  and  $\psi(x, t)$  determined by Eq. (8) may not be expressed through the rudimentary functions as that shown in Eqs. (16), (19), (21) and (24), but the analytical formulation  $G(x, t)$  and  $\psi(x, t)$  can be of bright soliton type as well as dark soliton type (through appropriate signs setting of  $g_1$ ,  $g_2$  and  $g_3$ ). The soliton features under such scenario may require partial numerical evaluation. We will see later that the analytical soliton solution for the cubic-quintic-septic case gives rather precise description of the sonic horizon dynamics of the quantum system under investigation.

### III. SOLITON EVOLUTION FOR THREE DIMENSIONAL NLSE WITH CUBIC-QUINTIC-SEPTIC NONLINEARITY

To study the sonic horizon dynamical behavior for actual quantum system setting, we need to consider the more general three-dimensional scenario. The three-dimensional NLSE with specific cubic-quintic-septic nonlinearity is formulated as follow

$$i \frac{\partial}{\partial t} \psi = [-\nabla^2 + kr^2 + (g_1 |\psi|^2 + g_2 |\psi|^4 + g_3 |\psi|^6)] \psi. \quad (25)$$

To derive the analytical solutions for the above Eq. (25), we use the self-similar approach based on the developed one-dimensional soliton solutions of the 1D NLSE model (also with cubic-quintic-septic nonlinearity). To eliminate any integrable constraint in the solution analysis process of the three-dimensional NLSE, we also introduce a parametric function  $\varpi(t)$  similar to  $\sigma(t)$  in the one-dimensional case, and similar to the 1D NLSE case, the associated transformation takes the following form

$$\mathbf{r}' = \varpi(t') \mathbf{r}, \quad (26a)$$

$$t' = \int \varpi^2(t) dt. \quad (26b)$$

We then assume that the wave function transforms as follow,

$$\psi(\mathbf{r}, t) = \varpi^{3/2}(t') \exp\left[-\frac{i}{4} \frac{\varpi'(t')}{\varpi^3(t')} \sum_j x_j'^2\right] \varphi(\mathbf{r}', t'). \quad (27)$$

Switching notations from  $(\mathbf{r}', t')$  to  $(\mathbf{r}, t)$ , Eq. (25) now takes the following form:

$$i\varphi_t + \Delta \varphi + (s_0(t) |\varphi|^2 + s_1(t) |\varphi|^4 + s_2(t) \nabla^2 \varphi) \varphi + \omega(t) r^2 \varphi = 0, \quad (28)$$

with  $s_i(t) = g_i(t) \varpi^{2i+2}(t)$  ( $i = 0, 1$ ),  $s_2(t) = g_2 \varpi^3(t)$ , and  $\omega(t) = \{4k(t) + \varpi_t^2(t)/\varpi^5(t) - [\varpi_t(t)/\varpi(t)]_t\} / [4\varpi^4(t)]$ . The general (1+1) self-similar projective equation for the 3D NLSE (25) takes the following form

$$iu_\tau + \epsilon u_{\zeta\zeta} + k'(t) \zeta^2 + (\delta_1 |u|^2 + \delta_2 |u|^4 + \delta_3 |u|^6) u = 0, \quad (29)$$

which is equivalent to Eq. (1) only with different notation for the parameters. Next, we choose the similarity ansatz for  $\varphi$  as follow:

$$\varphi(\mathbf{r}, t) = A(t) u[\zeta(\mathbf{r}, t), \tau(t)] \exp[ia(\mathbf{r}, t)], \quad (30)$$

where  $u(\zeta, \tau)$  is in the forms like Eqs. (16), (19) and (22) or other analytical solution format that might not expressible in rudimentary function form.

The implementation of the self-similarity approach, combined with the parametric function  $\varpi(t)$  will eliminate the traditional integrability constraints, as shown in the ensuing steps.  $A(t)$ ,  $\zeta(\mathbf{r}, t)$ ,  $\tau(t)$ , and  $a(\mathbf{r}, t)$  in expression (30) are functions of spatial and time coordinates to be determined in the ensuing steps. Substituting the ansatz (30) into Eq. (28) and formulating the obtained equation in the form of Eq. (29), we get a collection of relationship equations as follows

$$2s_0(t)A^2 - \delta_1 \tau_t = 0, \tag{31a}$$

$$2s_1(t)A^4 - \delta_2 \tau_t = 0, \tag{31b}$$

$$2s_2(t)A^2 - \delta_3 \tau_t = 0, \tag{31c}$$

$$\sum_j \zeta_{jj} = 0, \tag{31d}$$

$$\sum_j \zeta_j^2 - \varepsilon \tau_t = 0, \tag{31e}$$

$$\zeta_t + 2 \sum_j \zeta_j a_j = 0, \tag{31f}$$

$$2A_t + 2A \sum_j a_{jj} = 0, \tag{31g}$$

$$a_t + a_x^2 + a_y^2 + a_z^2 - (\omega(t) + k'(t)) \sum_j x_j^2 = 0, \tag{31h}$$

Eqs. (31) are solvable via parametric function  $\varpi(t)$  introduced. The analytical solutions of Eqs. (31) are,

$$A(t) = \sqrt{\frac{3\delta}{\varepsilon s}} G, \tag{32a}$$

$$\zeta(\mathbf{r}, t) = -6D_1 \int G^2 dt + G \sum_j x_j + D_2, \tag{32b}$$

$$\tau(t) = \frac{3}{\varepsilon} \int G^2 dt + D_3, \tag{32c}$$

$$a(\mathbf{r}, t) = \frac{s_t}{4s} \sum_j x_j^2 + D_1 G \sum_j x_j - 3D_1^2 \int G^2 dt + D_4, \tag{32d}$$

Here  $s(t) = s_0(t)$ ,  $j = x, y, z$ ,  $G = \exp[-\int s_t / s dt]$  and  $D_{1,2,3,4}$  are constants after integration. The self-consistence equation eliminates the integral constraint via the introduction of  $\varpi(t)$  and takes the following form

$$\frac{s_{tt}}{s} - 4(\omega(t) + k'(t)) = 0. \tag{33}$$

where the functions  $s_i(t)$  ( $i = 0, 1, 2$ ) and  $\omega(t)$  depend on  $\varpi(t)$ , Eq. (33) is just the equation for  $\varpi(t)$ , making  $g_i(t)$  ( $i = 1, 2, 3$ ) and  $k(t)$  acting as free parametric functions. Combined with Eq. (33), The solution (30) gives the analytical soliton solution of the 3D NLSE (25) with cubic-quintic-septic nonlinearity, from which the sonic horizon dynamics can be calculated in a more general manner.

#### IV. SONIC HORIZON FORMATION FOR THE SYSTEM MODELED BY CUBIC-QUINTIC-SEPTIC NONLINEARITY

Now we proceed with the analysis of sonic horizon formation for the elongated system modeled with cubic-quintic-septic nonlinearity. In section II, we see that the soliton feature is clearly shown through the solution modulus of the wave function of Eq. (1). The phase function  $\theta(x, t)$  contains the kinetic motion information of the system. From Eq. (9),  $p(t)$  is expressed by  $\sigma(t)$  in Eq. (10a), so  $\Phi_2(t)$  is expressed by  $\sigma(t)$  from Eq. (9g) and  $\Phi_1(t)$  is expressed by  $\sigma(t)$  in Eq. (9b). These demonstrate that parametric functions  $\Phi_2(t)$  and  $\Phi_1(t)$  depend on  $\sigma(t)$  (so that  $\Phi_2(t) = \frac{\dot{\sigma}(t)}{2\sigma(t)}$ ,  $\Phi_1(t) = C_1/\sigma(t)$ ). The equation for  $\sigma(t)$  is formulated (from Eqs. (10a), (9g), and (9a)) as:

$$\frac{d}{dt} \left( \frac{\dot{\sigma}}{\sigma^3} \right) + 4 \frac{\dot{\sigma}^2}{\sigma^4} + \frac{k}{\sigma^2} - \left( \frac{\dot{\sigma}}{2\sigma} \right)^2 + \frac{d}{dt} \left( \frac{\dot{\sigma}}{4\sigma} \right) = 0 \tag{34}$$

Eq. (34) has the following solution

$$\rho(t) = \sqrt{A_0 + B_0 \sin \omega t} \tag{35}$$

where  $\sigma_0$ ,  $C_1$ , and  $C_2$  are integral constants,

$$\omega = 2\sqrt{\frac{k}{m}}, \tag{36}$$

$$A_0 = \sqrt{\left( \frac{\sigma_0^2}{2} + \frac{\hbar^2}{4m_a k \sigma_0^2} \right)^2 - \frac{C_2 \hbar^2}{4C_1 m_a k}}, \tag{37}$$

$$B_0 = \frac{\sigma_0^2}{2} + \frac{C_2 \hbar^2}{4C_1 m_a k \sigma_0^2} \tag{38}$$

We note that in the definition of  $\theta(x, t)$ ,  $x$  is  $x' = \sqrt{\frac{2m\omega}{\hbar}} \sigma(t') x$ . The analytical expression for the system's flow velocity is

$$v(x, t) = \frac{\partial \theta(x', t)}{\partial x} = 2\Phi_2(t)\sigma^2(t)x + \Phi_1(t)\sigma(t) = \frac{\dot{\sigma}(t)}{2\sigma(t)} x + C_1, \tag{39}$$

Fig. 3 shows that the theoretically derived flow velocity (with full cubic-quintic-septic nonlinearity) in comparison with the corresponding velocity value from numerical analysis. Based on the actual definition of the system flow velocity, the numerical system flow

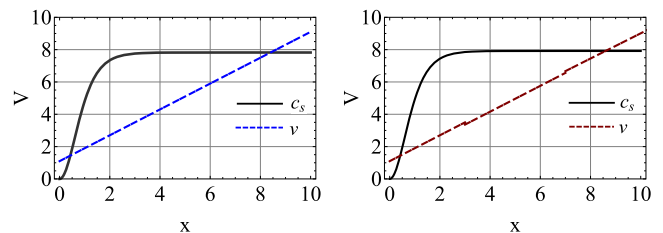


FIG. 3. Plots of the system flow velocity  $v$  vs.  $x$  (dashed line) from theoretical derivation (left) and numerical analysis (right).  $c_s$  (solid line) is the sound velocity, which is proportional to the modulus of the system wave function.

velocity is generated by the gradient calculation of the phase function of the numerically generated wave function. The numerical wave function is generated from the same initial setting (initial wave function) at time  $t = 0$  as that for the analytically derived wave function at  $t = 0$ . The cross point between the flow velocity curve and the sound velocity curve indicates the location of the sonic horizon. From Eq. (39), we can see that the flow velocity is time dependent, so that the occurrence and the spatial location of the sonic horizon are also time dependent. Moreover, for Fig. 3, we see that the agreement between our derived flow velocity and the numerical calculated distribution is very good, demonstrating the applicability of our theoretical treatment presented here for NLSE with cubic-quintic-septic nonlinearity.

## V. CONCLUSION

In this study, the sonic horizon formation problem for quantum system incorporating cubic-quintic-septic nonlinearity is investigated based on the analytical study of the NLSE model with nonlinearity up to septic order. Via the F-expansion method combined with coupled modulus-phase transformation, we derived the soliton solution for the NLSE with cubic, quintic, and septic nonlinearity respectively for the one-dimensional case first. Based on the self-similar approach, we then derived the soliton solution for the three-dimensional NLSE, showing the typical nonlinear feature of the septic nonlinear media. The analytical results obtained allowed us to calculate the sonic formation dynamics and derive the key system kinetic variables. We show that the sonic horizon formation location from our derived system flow velocity and sound velocity agrees very well with those obtained from pure numerical analysis, demonstrating the applicability of our theoretical approach. The analytical results derived in this work can be used to guide relevant experimental study for sonic horizon formation in system with septic nonlinearity.

## ACKNOWLEDGMENTS

This work was supported by the National Natural Science Foundation (NSF) of China under grant nos. 11547024, 11874185.

## REFERENCES

- <sup>1</sup>W. G. Unruh, *Phys. Rev. Lett.* **46**, 1351 (1981).
- <sup>2</sup>J. Steinhauer, *Nature Phys.* **12**, 959–965 (2016).
- <sup>3</sup>L. J. Garay, J. R. Anglin, J. I. Cirac, and P. Zoller, *Phys. Rev. Lett.* **85**, 4643 (2000).
- <sup>4</sup>Y. Wang and S. Y. Zhou, *AIP Advances* **7**, 085006 (2017).
- <sup>5</sup>Y. Wang and Y. Yang, *AIP Advances* **8**, 095317 (2018).
- <sup>6</sup>C. Zhan, D. Zhang, D. Zhu, D. Wang, and Y. Nie, *J. Opt. Soc. Am. B* **19**, 369 (2002).
- <sup>7</sup>R. A. Ganeev, M. Baba, M. Morita, A. I. Ryasnyansky, M. Suzuki, M. Turu, and H. Kuroda, *J. Opt. A: Pure Appl. Opt.* **6**, 282 (2004).
- <sup>8</sup>B. Gu, Y. Wang, W. Ji, and J. Wang, *Appl. Phys. Lett.* **95**, 041114 (2009).
- <sup>9</sup>F. Smektala, C. Quemard, V. Couderc, and A. Barthlmy, *J. Non-Cryst. Solids* **274**, 232 (2000).
- <sup>10</sup>G. S. Agarwal and S. Dutta Gupta, *Phys. Rev. A* **38**, 5678 (1988).
- <sup>11</sup>Y. Kurita and T. Morinari, *Phys. Rev. A* **76**, 053603 (2007).
- <sup>12</sup>A. X. Zhang and J. K. Xue, *Chin. Phys. Lett.* **25**, 39 (2008).
- <sup>13</sup>H. Liu, D. H. He, S. Y. Lou, and X. T. He, *Chin. Phys. Lett.* **26**, 120308 (2009).
- <sup>14</sup>S. Zhang, J. M. Ba, Y. N. Sun, and L. Dong, *Z. Naturforsch.* **64a**, 691–696 (2009).
- <sup>15</sup>J. X. Fei and C. L. Zheng, *Chin. J. Phys.* **51**, 200 (2013).
- <sup>16</sup>C. Trallero-Ginera, J. C. Drake-Pereza, V. Lopez-Richardb, and J. L. Birmanc, *Physica D* **237**, 2342 (2008).
- <sup>17</sup>R. Atré, P. K. Panigrahi, and G. S. Agarwal, *Phys. Rev. E* **73**, 056611 (2006).
- <sup>18</sup>Y. S. Cheng, H. Li, and R. Z. Gong, *Chin. Opt. Lett.* **3**, 715–718 (2005).
- <sup>19</sup>H. Li and D. N. Wang, *Chin. Opt. Lett.* **6**, 611–614 (2008).
- <sup>20</sup>B. A. Malomed, D. Mihalache, F. Wise, and L. Torner, *J. Opt. B: Quantum Semiclass. Opt.* **7**, R53 (2005).
- <sup>21</sup>P. Grelu, J. M. Soto-Crespo, and N. Akhmediev, *Opt. Express* **13**, 9352 (2005).
- <sup>22</sup>Y. Wang, Y. Yang, S. Q. He, and W. Wang, *AIP Advances* **7**, 105209 (2017).
- <sup>23</sup>Y. Zhou, M. L. Wang, and Y. M. Wang, *Phys. Lett. A* **308**, 31 (2003).
- <sup>24</sup>M. A. Abdou, *Chaos, Solitons and Fractals* **31**, 95 (2007).
- <sup>25</sup>Y. Wang and Y. Zhou, *AIP Advances* **4**, 067131 (2014).